

# VOUGHT-SIKORSKY AIRCRAFT LIBRARY

TECHNICAL NOTES

NATIONAL ADVISORY COMMITTEE FOR AERONAUTICS

---

No. 747

---

PROPELLER ROTATION NOISE DUE TO TORQUE AND THRUST

By Arthur F. Deming  
Langley Memorial Aeronautical Laboratory

---

Washington  
January 1940

# NATIONAL ADVISORY COMMITTEE FOR AERONAUTICS

## TECHNICAL NOTE NO. 747

### PROPELLER ROTATION NOISE DUE TO TORQUE AND THRUST

By Arthur F. Deming

#### SUMMARY

Sound pressures of the first four harmonics of rotation noise from a full-scale two-blade propeller were measured and are compared with values calculated from theory. The comparison is made (1) for the space distribution with constant tip speed and (2) for fixed space angles with variable tip speed.

A relation for rotation noise from an element of radius developed by Gutin is extended to cover the entire propeller disk. Curves are given showing the effect of number of blades on the rotation noise.

#### INTRODUCTION

Propeller noise can, in general, be divided into two classifications: (1) rotation noise and (2) vortex noise. The first is by far the more intense. The second, as the name implies, is due to the shedding of vortices from the blades; and its intensity and frequency spectrum probably depend on angle of attack, velocity, air turbulence, blade chord, and shape of the blade sections from hub to tip.

The rotation noise is due to the pressure wave enveloping each blade and moving with it; the vortex noise is due to pressure variations on the blade as a result of variations of circulation. It may be simply stated that the rotation noise is due to the constant air force on the blades and that the vortex noise is due to the vortices shed in the wake.

The rotation noise may be further divided into the rotation noise due (1) to torque and thrust and (2) to blade thickness. The second case has been treated in a previous paper (reference 1). The effect of thickness on rotation noise is small except for the higher harmonics and small angles of attack.

The propeller rotation-noise theory (reference 2) does not check with experiment in some respects, especially in the details of spatial distribution and time phase of the harmonics; but the theory does predict to a fair degree of accuracy the energy radiated as sound and the maximum sound pressures encountered. The general shape of the spatial distribution of sound pressure of the fundamental and the second harmonic for a two-blade propeller is fairly well given by theory. For higher harmonics, the distribution is not so well given by theory. The use of the theory does, however, give relatively accurate values for the magnitudes to be expected, which is perhaps all that is required in sound research where one is dealing with sound levels in decibels instead of percentages.

#### THEORY OF EFFECT OF TORQUE AND THRUST

Gutin (reference 2) starts his derivation for the effect of torque and thrust with

$$\phi = - \frac{i}{4\pi k \rho c} \left( X \frac{\partial}{\partial x} + Y \frac{\partial}{\partial y} + Z \frac{\partial}{\partial z} \right) \frac{e^{-ikr}}{r} \quad (1)$$

and arrives at the result

$$P = \frac{m \omega_1}{2\pi c r} \left[ -P \cos \vartheta + \frac{n c M}{\omega_1 R^2} \right] J_{mn} (kR \sin \vartheta) \quad (2)$$

Equation (1) employs the standard notation used in acoustics,  $X$ ,  $Y$ , and  $Z$  being the components of force exerted by the blade element on the medium. Some of the symbols used by Gutin are different from those used by the N.A.C.A. in acoustics; in order to avoid confusion, the following table, which compares acoustic symbols, has been included in this paper.

Item	Gutin	N.A.C.A.
Mass density of medium	$\rho$	$\rho$
Velocity of sound	$c$	$c$
Angular velocity	$\omega, (\omega_1 = n\omega)$	$\omega = \frac{V}{R}$
Frequency, cycles per second	$f$	$f$
Wave length	$\lambda$	$\lambda$
Distance of microphone to center of propeller	$r$	$l$
Number of blades	$n$	$n$
Order of harmonic	$m$	$q$
Thrust	$P$	$T$
Total thrust	$P$	$T_0$
Torque	$M$	$Q$
Total torque	$M$	$Q_0$
Propeller radius	$R$	$R$
Propeller tip radius	$R_0$	$R_0$
Blade-element station	--	$x = \frac{R}{R_0}$
Section velocity	--	$V$
Angle in disk from reference	$\theta$	$\theta$
Direction from front of disk	$\vartheta$	$\beta$
Bessel function argument	$kR \sin \vartheta$	$m = qn \sin \beta \frac{V}{c}$
Sound pressure	$P$	$P_{qn}$
Harmonic power, watts	$W$	$P_{qn}$
Constants	--	$K_T, K_Q$

Item	Gutin	N.A.C.A.
Solidity	--	$\sigma$
Distribution exponent	--	a, b, c, and f
Bessel function of first kind of order $qn$	$J_{mn}$	$J_{qn}$

Gutin, in the course of his derivation of equation (2), develops the relation for the sound pressure at a distant point due to the torque and the thrust from an element of radius  $dR$ . This relation, expressed in the N.A.C.A. acoustic notation, is

$$dp_{qn} = \frac{qmw}{2\pi cl} \left( -\frac{dT}{dR} \cos \beta + \frac{c}{\omega R^2} \frac{dQ}{dR} \right) J_{qn}(m) dR \quad (3)$$

From this relation, Gutin, by studied approximations, arrives at the relation given in equation (2).

The use of simple relations to represent the torque and the thrust distribution makes it quite feasible to integrate over the entire disk. An equation resulting from this integration will show the effect of torque and thrust distribution on the sound pressure of the harmonic components.

By the use of

$$\frac{dT}{dR} = K_T \left[ \left( \frac{R}{R_0} \right)^a - \left( \frac{R}{R_0} \right)^b \right] \quad (4)$$

and

$$\frac{dQ}{dR} = K_Q \left[ \left( \frac{R}{R_0} \right)^c - \left( \frac{R}{R_0} \right)^f \right] \quad (5)$$

for the thrust and the torque distributions, respectively, equation (3) can be integrated. The constants  $K_T$  and  $K_Q$  in equations (4) and (5) can be found by inte-

grating with respect to  $R$  from 0 to  $R_o$ . The result is

$$K_T = \frac{T_o}{R_o} \left[ \frac{(a+1)(b+1)}{(b-a)} \right] \quad (6)$$

and

$$K_Q = \frac{Q_o}{R_o} \left[ \frac{(e+1)(f+1)}{(f-e)} \right] \quad (7)$$

where the subscript  $o$  refers to the values at the tip and to integrated values.

Substitution of the values for  $\frac{dT}{dR}$  and  $\frac{dQ}{dR}$  in equation (3) gives

$$p_{qn} = \frac{qn\omega}{2\pi cl} \int_0^{R_o} \left\{ -\frac{T_o}{R_o} \cos \beta \frac{(a+1)(b+1)}{(b-a)} \left[ \left( \frac{R}{R_o} \right)^a - \left( \frac{R}{R_o} \right)^b \right] + \frac{cQ_o}{\omega R_o^2} \frac{(e+1)(f+1)}{(f-e)} \left[ \left( \frac{R}{R_o} \right)^e - \left( \frac{R}{R_o} \right)^f \right] \right\} J_{qn}(m) dR \quad (8)$$

Integration of equation (8) gives

$$p_{qn} = \frac{qn\omega}{2\pi cl} \left\{ -T_o \cos \beta (a+1)(b+1) \left[ \frac{1}{(qn+a+1)(qn+b+1)} - \frac{m_o^2}{2(2qn+2)(qn+a+3)(qn+b+3)} + \frac{m_o^4}{2 \times 4(2qn+2)(2qn+4)(qn+a+5)(qn+b+5)} - \dots \right] + \frac{cQ_o}{\omega R_o^2} (e+1)(f+1) \left[ \frac{1}{(qn+e+1)(qn+f+1)} - \frac{m_o^2}{2(2qn+2)(qn+e+3)(qn+f+3)} + \frac{m_o^4}{2 \times 4(2qn+2)(2qn+4)(qn+e+5)(qn+f+5)} - \dots \right] \right\} \frac{m_o^{qn}}{2^{qn}(qn)!} \quad (9)$$

where  $m_0 = qn \sin \beta \frac{V_0}{c}$ . It can be shown that the argument  $m_0$  is equal to  $\frac{2\pi R \sin \beta}{\lambda}$ , or the number of wave lengths contained in a distance equal to  $\pi$  times the diameter projected on the line to the observer.

Equation (8) could have been integrated in terms of a series of Bessel functions, for which tables could be used; but the expression resulting therefrom would be more cumbersome to use than equation (9), at least for the smaller values of  $qn$ .

#### REFERENCE CONDITIONS

The conditions under which the calculations for the sound pressures and the experimental tests were made are:

Number of propeller blades  $n$ , 2.

Blade radius to tip  $R_0$ , 4.75 feet.

Blade section, R.A.F. 6.

Blade angle at  $0.75R_0$   $\alpha$ ,  $5^\circ$ .

Distance of microphone to propeller center  $l$ , 85 feet.

Total thrust at propeller speed of 1,700 r.p.m.

$\left(\frac{V}{nD} = 0\right) T_0$ , 668 pounds.

Total torque at propeller speed of 1,700 r.p.m.

$\left(\frac{V}{nD} = 0\right) Q_0$ , 351 pound-feet.

Specific acoustic resistance  $\rho c$ , 42 grams per second centimeter<sup>2</sup>.

The data for the polar curves were obtained at a constant propeller speed of 1,700 r.p.m. and with the azimuth angle  $\beta$  between propeller axis and microphone changed in steps of  $15^\circ$ . For the speed runs, the angle was held at a constant value of  $120^\circ$  for the fundamental,  $110^\circ$  for the second and the third harmonics, and  $102-1/2^\circ$  for the fourth harmonic, while the speed was varied from minimum to maximum.

## COMPARISON OF EXPERIMENTAL AND CALCULATED SOUND PRESSURES

The calculated and the experimental sound pressures are compared for the first four harmonics of the sound for the reference conditions. The comparisons are for (1) the polar distribution of sound and (2) the variation of sound pressure with propeller speed for a fixed polar angle  $\beta$  from the propeller axis.

Figure 1 shows the variation of sound pressure with  $\beta$  for the first four harmonics. The polar distribution of the sound pressures is represented by three curves: one from experimental values, the second from values calculated from equation (2), and the third from equation (9). In equation (2),  $P$  and  $M$  are the total torque and thrust, respectively, and  $R = 0.75R_0$ . For use in equation (9),  $a = 2$ ,  $b = 12$ ,  $c = 2$ , and  $f = 12$  (see fig. 2); these parameters give the thrust and the torque distribution fairly well for the blade angle used with zero advance,  $V/nD = 0$ . It should be added that the theoretical values were multiplied by  $\sqrt{2}$  for plotting and for comparison with the experimental values. Because the microphone was on the ground, it was necessary to multiply the theoretical values by 2 and, because the equation gives maximum values, division by  $\sqrt{2}$  will give root-mean-square values for which the microphone is calibrated.

For the given directions or angles  $\beta$ , the  $\log_{10}$  of the sound pressure  $p_{qn}$  is shown plotted against  $\log_{10} V_0/c$  (speed runs) in figure 3. Figure 3(a) shows the experimental values; figure 3(b) shows the values obtained from equations (2) and (9). The mean slopes of these graphs are shown in figure 4 plotted against  $qn$ .

## EFFECT OF NUMBER OF BLADES

Notice that, in the formulas,  $q$  and  $n$  appear only as the product  $qn$ . Thus the sound pressure of a certain frequency is the same whether the fundamental of a four-blade propeller or the second harmonic of a two-blade propeller is concerned, provided that the total thrust and torque are the same. Note that only multiples of the fundamental of each propeller occur.



Figure 5 shows the sound pressure  $p_{qn}$  plotted against  $qn$  for the reference conditions given earlier with the thrust and the torque fixed. It will be realized the  $qn$  must be a whole number; obviously, values between whole numbers have no practical meaning.

For a two-blade propeller, the values of  $qn$  for the harmonics would be 2, 4, 6, 8, 10, 12, etc.; for a three-blade propeller, 3, 6, 9, 12, 15, 18, etc.; for a four-blade propeller 4, 8, 12, 16, 20, 24, etc.. For any value of tip speed used, the sound pressure of all the harmonics for any condition can be estimated from curves like those in figure 5. It must be remembered that the sound pressure is proportional to the torque and the thrust as shown in equation (9) and that figure 5 is plotted for the given conditions with  $\beta = 110^\circ$ .

#### POWER RADIATED AS ROTATION NOISE

For normal conditions, the power radiated as sound is largely made up of rotation noise. The power involved in the vortex noise is relatively small except at low values of  $V_0/c$ . This conclusion would be true for propellers with two or three blades; it is possible, however, that the power involved in vortex noise may be equal to or even greater than that due to rotation noise for a large number of blades.

The power in watts radiated can be obtained by substituting the data given herein in the relation (see reference 2)

$$P_{qr} = \frac{10^{-7}}{\rho c} \int_0^\pi \frac{p_{qn}^2}{2} 2\pi r^2 \sin \beta \, d\beta \quad (10)$$

For this relation, the data given by the polar curves of the sound pressures can be used. These data were measured at 15 intervals up to  $360^\circ$ , making 24 values for the complete polar circle. Since sound pressures were measured on both sides of the  $0^\circ - 180^\circ$  axis, the square of each pressure measured from  $0^\circ$  to  $180^\circ$  should be added to the square of the corresponding pressure on the opposite side of the axis and the mean of these two squares be taken. This computation will result in 12 values of  $p_{qn}^2$  for the experimental sound pressure consistent with the range of the integral 0 to  $\pi$ . An important fact to remember is

that the values of  $p_{qn}$  used in equation (10) refer to the values of  $p_{qn}$  calculated from equations (2) and (9), which are maximum values of the sinusoidal sound pressures calculated for free space. The sound pressures measured by the microphone on the ground are double the values that would be measured in the same relative locations in free space. If values were taken from figure 1, they must therefore be divided by  $\sqrt{2}$ . Equation (10) then becomes, with  $p_{qn}$  as the measured pressures,

$$P_{qn} = \frac{\pi^2 \cdot 10^{-7}}{2 \times 12\pi c} \sum_0^{12} P_{qn}^2 \sin \beta \quad (11)$$

The values of  $p_{qn}$  were obtained for the first four harmonics  $qn = 2, 4, 6$ , and  $8$ , by three methods: (1) from the experimental data; (2) from equation (2); (3) from equation (9) with  $x^2 - x^{12}$  used for the thrust and the torque distribution. All other reference conditions were the same. The calculations of the power radiation, expressed in watts, are compared in the following table:

	Experimental data	Equation (2)	Equation (9)
$P_{1 \times 2}$	18.2	17.0 8.5	14.8 7.4
$P_{2 \times 2}$	6.3	5.6 2.8	5.2 2.6
$P_{3 \times 2}$	2.9	1.6 .8	2 1.0
$P_{4 \times 2}$	1.2	.4 .2	.7 .35

These listed values of power radiated by the first four harmonics are plotted on semilog paper in figure 6.

The sum of the wattages for the first four harmonics gives very nearly the total power in the rotation noise. From the three different methods of calculation, the powers are

$$\text{Experiment,} \quad \sum_{qn=2}^8 P_{qn} = 28.7 \text{ watts.}$$

$$\text{Equation (2),} \quad \sum_{qn=2}^8 P_{qn} = 12.3 \text{ watts, } 3.68 \text{ decibels below } 28.7 \text{ watts.}$$

$$\text{Equation (9),} \quad \sum_{qn=2}^8 P_{qn} = 11.3 \text{ watts, } 4.04 \text{ decibels below } 28.7 \text{ watts.}$$

#### DISCUSSION

In the course of the experimental work connected with this paper, the question of interference appeared. With the microphone placed 5 feet above the ground, data were obtained that gave speed-run curves which were less steep than theory indicated, particularly for the third and the fourth harmonics. The polar curves obtained with the microphone in this position did, however, check reasonably well with the theory.

With the microphone on the ground, the position used for the data presented herein, the slopes of the speed-run curves were steeper than theory indicated except that for the fourth harmonic, which was less steep than the theory indicated. This result is shown in figure 4. The slopes shown in figure 4 obtained from equations (2) and (9) are very nearly the same. The polar curves give a fair check for the first and the second harmonics, but the third and the fourth harmonics show a discrepancy of about 4.6 and 6.4 decibels, respectively, for power radiated.

As might be expected, the first harmonic showed little effect of interference because the wave length was about 20 feet for a propeller speed of 1,700 r.p.m. This wave length was sufficiently large compared with the mesh of the

nearby objects and the roll of the ground that the acoustic image of the propeller was fairly definite but was probably not definite enough for the higher harmonics.

As has probably been observed, the curves obtained from equations (2) and (9) do not check in absolute magnitude. For the first and the second harmonics, the use of equation (2) results in the higher values, giving the better check of theory with experiment. The opposite is true for the third and the higher harmonics because equation (9) gives the larger values. In equation (2), however,  $0.75R_0$  was used for  $R$  for all harmonics; whereas, progressively larger values should have been used for the higher harmonics. If larger values of  $R$  had been used in equation (2), as Gutin suggests in his studied approximations, the difference in sound pressures obtained from equations (2) and (9) would have been small.

As higher harmonics and a greater number of blades are considered, the thickness effect becomes more important relative to the thrust and the torque effect, particularly at high  $V_0/c$ . This conclusion is drawn from a study of the effect of  $q$  and  $n$  in equations (2) and (9) compared with the effect of  $q$  and  $n$  in equation (19) of reference 1.

A better approach to experimental data can be obtained by including thickness effect than from equation (2) or (9) alone. If the square root of the sum of the squares of the sound pressures obtained from equation (9) and from equation (19) of reference 1 were calculated, better comparison with experiment should result. A difference in time phase occurs between the thickness effect and the thrust and torque effect, the Fourier series for the thickness effect being a sine series and that for the thrust and torque effect being a cosine series; hence, the square root of the sum of the squares is suggested.

For convenience, equation (19) of reference 1 for thickness effect is repeated as equation (12) of this paper.

$$p_{qn} = 2\sqrt{2} \, qn \, a_{qn} f(a, b) \frac{R_0}{1} \frac{\rho_0}{2} \frac{V_0^2}{2^{qn}(qn)!} \frac{m_0^{qn}}{[qn+1]} \left[ \frac{1}{2(2qn+2)(qn+3)} + \frac{m_0^4}{2 \times 4(2qn+2)(2qn+4)(qn+5)} - \dots \right] \quad (12)$$

where

$$a_{qn} = \frac{qn^2 b^2}{4\pi R_0^2}$$

$$f(a,b) = \frac{8}{3} \frac{a}{b} \quad (\text{for typical symmetrical airfoil section}).$$

$a$  is one-half maximum thickness at about  $0.80R_0$ .

$b$ , chord at about  $0.80R_0$ .

and all of the other symbols are the same as those used in the present paper. As equation (12) gives twice the free-space root-mean-square values, all values obtained from equation (12) must be divided by  $\sqrt{2}$  in order to be used with the values obtained from equation (2) or (9).

The question of solidity  $\sigma$  is of importance in determining the Fourier coefficients; for the approximations made in deriving equations (2), (3), and (12), the angle  $qnb/R$  must therefore be reasonably small. If  $qnb/R$  is not small, errors in the calculation of  $p_{qn}$  will arise; but it is believed that harmonics up to the order of  $1/2\sigma$ , one-half the reciprocal of the solidity, can be calculated by equations (2), (9), and (12) without serious error from this cause. The solidity  $\sigma$  can be expressed by  $nb/2\pi R$ .

A good descriptive article by M. F. Dowell on the question of vortex noise (reference 3) recently appeared as a result of some investigations of fan noise. This work involved low tip speeds so that practically all of the noise generated was due to vortices trailing from the blades. If sufficiently high values of tip speed had been used in the tests, rotational noise would have had to be considered and would have dominated the acoustic spectrum from the fan. The importance of the rotation noise at high tip speeds is due to the fact that rotation noise generally increases with a greater power of  $V_0/c$  than does vortex noise. It is found from figure 4 that rotation noise power radiated in the harmonics varies approximately as the  $6 + 5/3$  power of  $V_0/c$ , but the power radiated as vortex noise varies as approximately the 5.5 power of  $V_0/c$  (reference 4).

## CONCLUSIONS

1. The theory gives values of total power radiated in the first four harmonics within 4 decibels of experimental values.

2. This study shows that the experimental results are in reasonably good agreement with Gutin's theory. The agreement is particularly good for the lower harmonics, in regard to both magnitude and distribution.

3. For the fourth harmonic, the results differ by as much as 8 decibels. This disagreement might be due to disregard of the thickness effect, which, in general, should be greater for the higher harmonics.

4. It has been shown that the power output in rotation noise increases as the  $6 + 5/3$  power of the tip speed.

5. The sound calculated by use of the  $x^2 - x^{12}$  distribution checks reasonably well with the sound calculated by Gutin's formula using  $0.75R_0$  as representative.

Langley Memorial Aeronautical Laboratory,  
National Advisory Committee for Aeronautics,  
Langley Field, Va., November 27, 1939.

## REFERENCES

1. Deming, A. F.: Noise from Propellers with Symmetrical Sections at Zero Blade Angle, II. T.N. No. 679, N.A.C.A., 1938.
2. Gutin, L.: Über das Schallfeld einer Rotierenden Luftschraube. Phys. Zeitschr. der Sowjetunion, Bd. 9, no. 1, 1936, pp. 57-71.
3. Dowell, M. F.: A Study of Air Movement through Axial-Flow Free-Air Propellers. Gen. Elec. Rev., vol. 42, no. 5, May 1939, pp. 210-17.
4. Stowell, E. Z., and Deming, A. F.: Vortex Noise from Rotating Cylindrical Rods. T.N. No. 519, N.A.C.A., 1935.

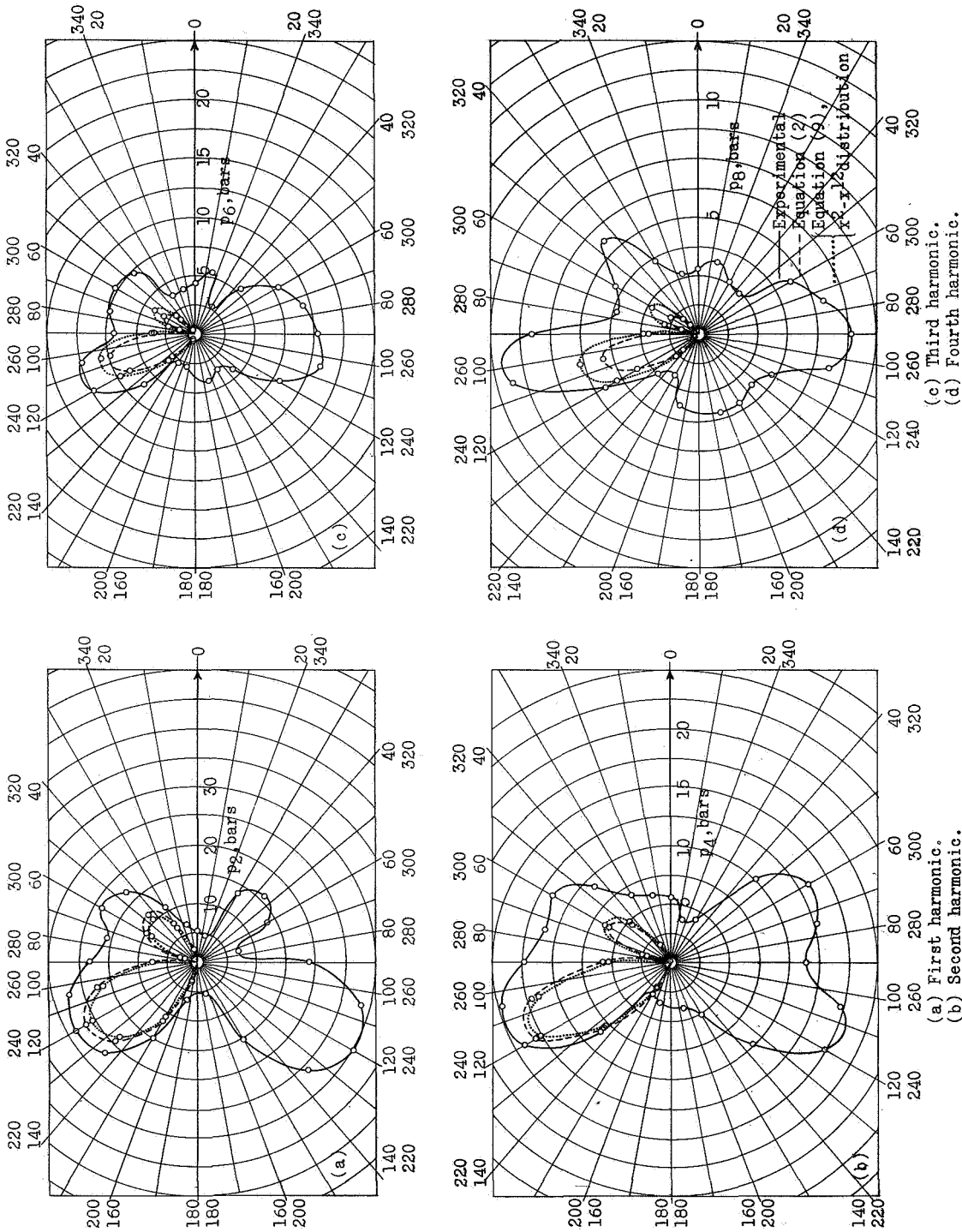


Figure 1, a to d.-The variation of sound pressure with  $\beta$  for the first four harmonics.



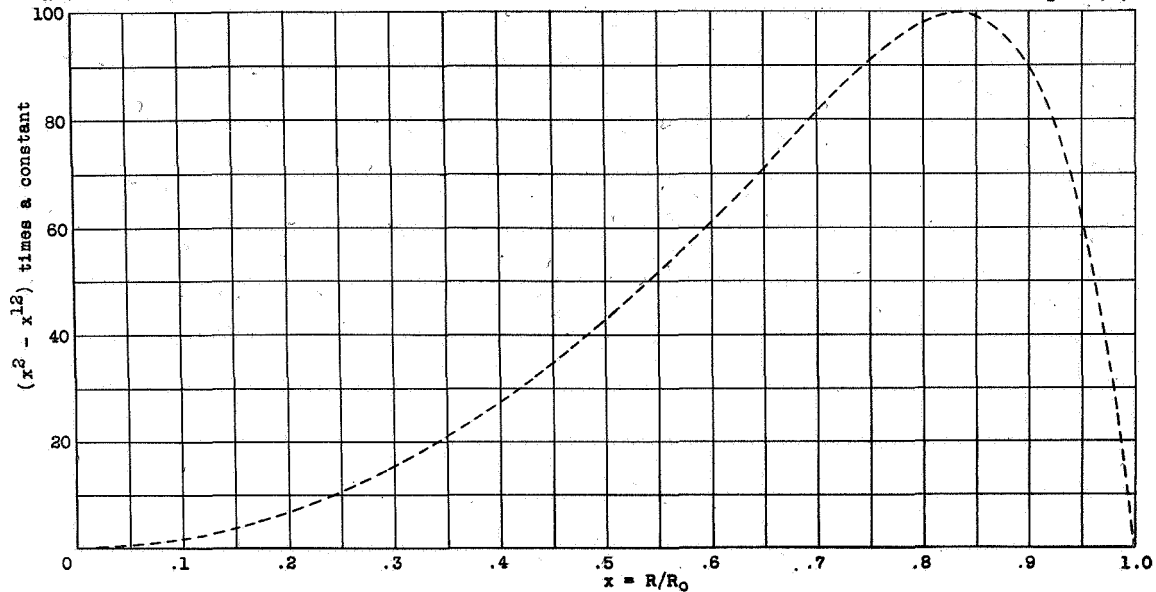


Figure 2.- Plot of  $(x^2 - x^{12})$  times a constant.

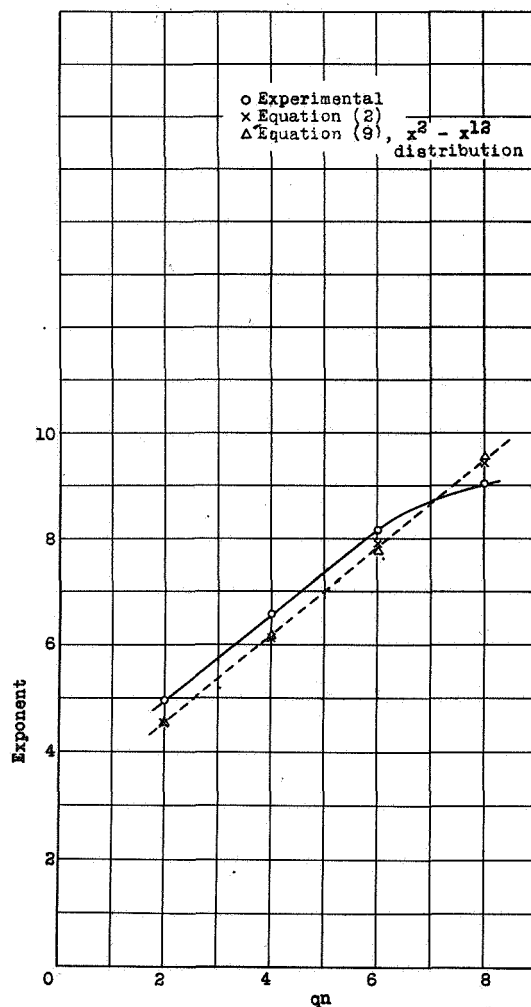


Figure 4.- Variation of the exponent of  $V_0/c$  with  $qn$ .

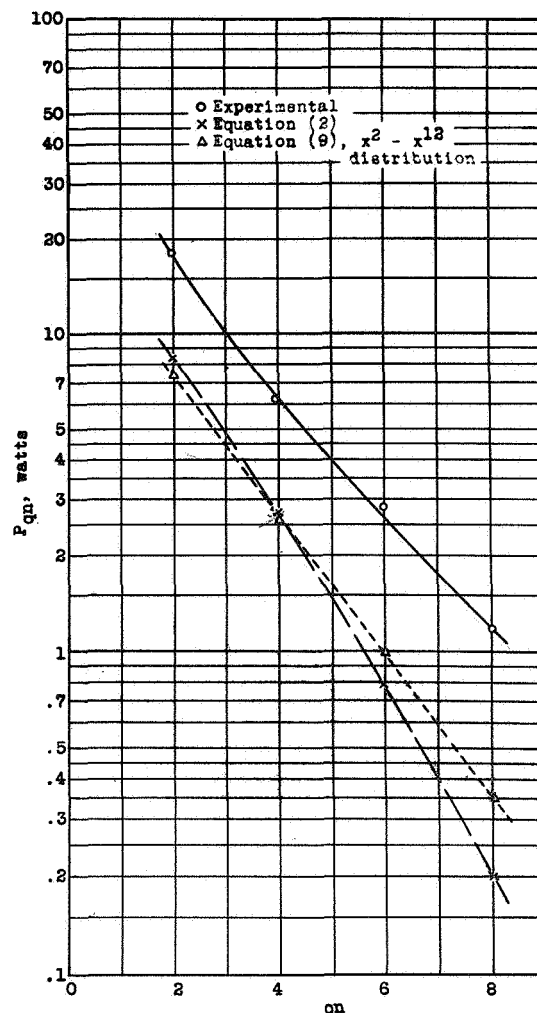


Figure 6.- Variation of  $P_{qn}$  with  $qn$  for the first four harmonics. Values obtained from experimental data, equation (2), and equation (9) for the reference conditions.

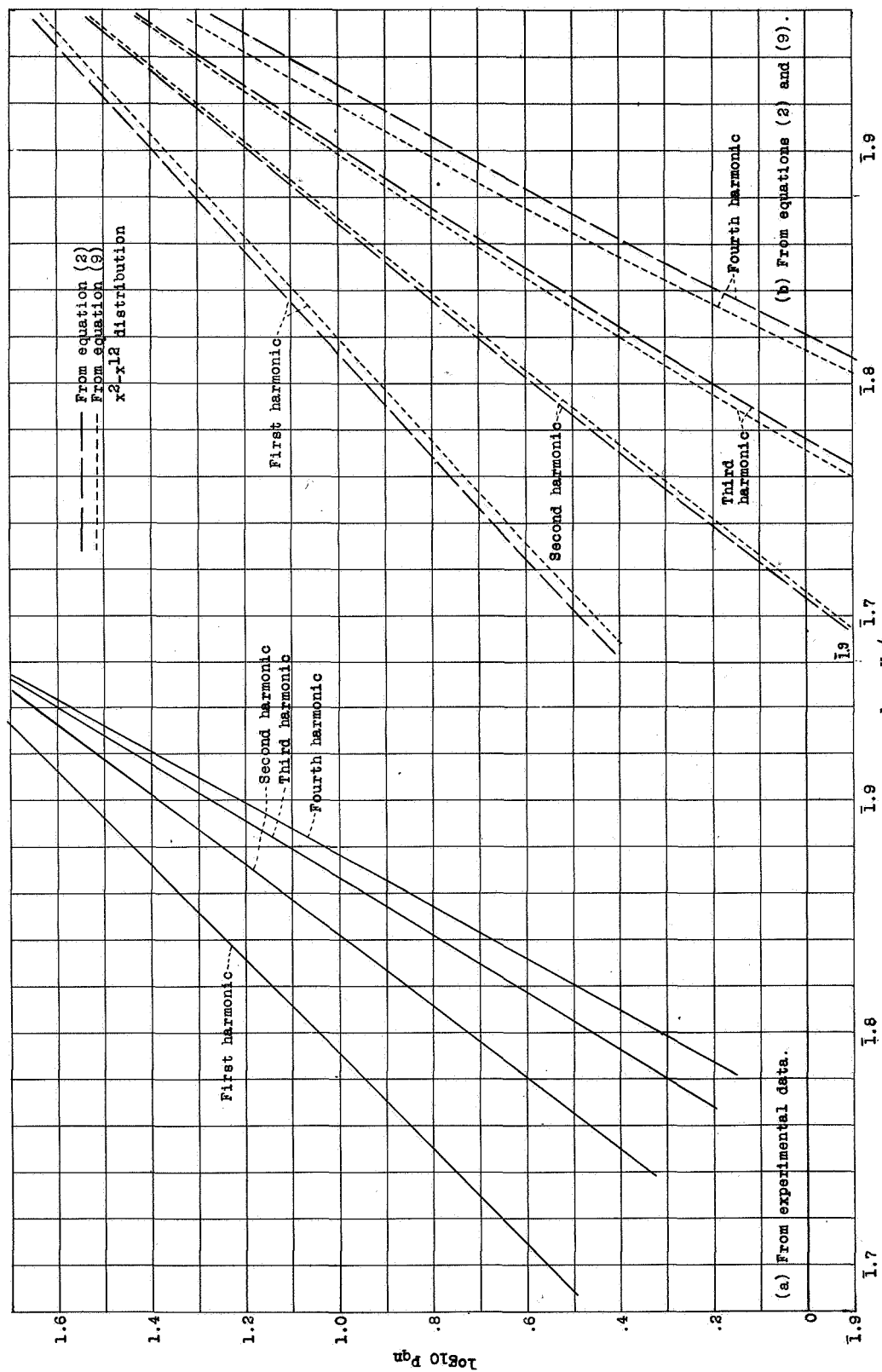


Figure 3.- Variation of  $\log_{10} p_{gn}$  with  $\log_{10} V_0/c$ .

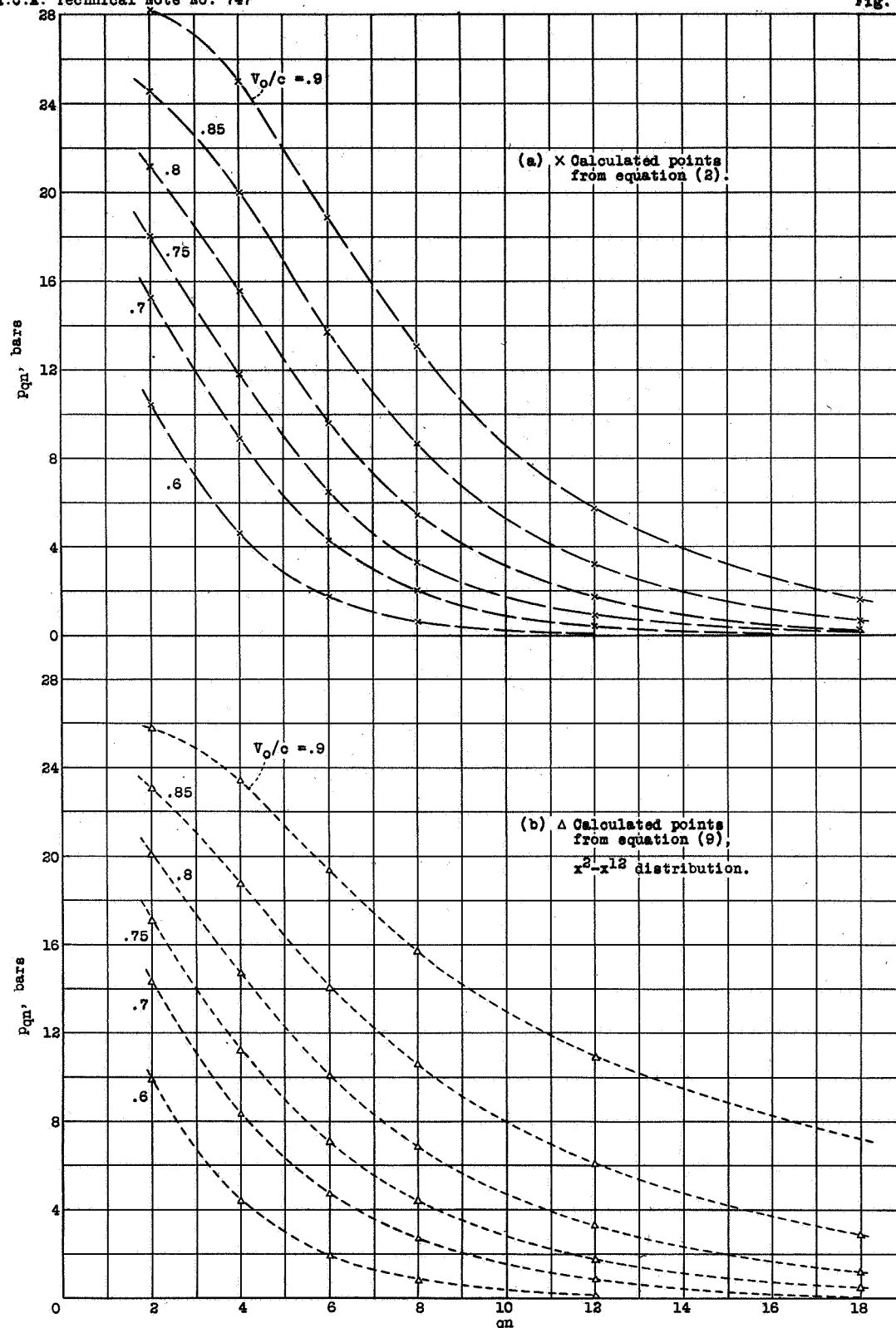


Figure 5.- Variation of  $P_{qn}$  with  $qn$  for six values of  $V_0/c$  at  $\beta = 110^\circ$ . Thrust and torque constant at given reference condition.